Microstructure and Solvent Distribution in Cross-Linked Diblock Copolymer Gels

D. A. Durkee,[†] E. D. Gomez,[†,‡] M. W. Ellsworth,[#] A. T. Bell,*[,†,⊥] and N. P. Balsara*[,†,‡,§]

Department of Chemical Engineering, University of California, Berkeley, California 94720; Materials Sciences Division, Environmental Energy Technologies Division, and Chemical Sciences Division, Lawrence Berkeley National Laboratory, University of California, Berkeley, California 94720; and Tyco Electronics Corporation, Menlo Park, California 94025

Received December 22, 2006; Revised Manuscript Received April 20, 2007

ABSTRACT: Gels were created by irradiating poly(α-methylstyrene-*block*-isoprene) (PaMS−I) and poly(vinylferrocenium triflate-*block*-isoprene) (PVFT−I) copolymers with an electron beam and swelling the resulting cross-linked solids in good solvents. The radiation cross-links the polyisoprene (PI) block, induces chain scission of the poly(α-methylstyrene) block (PaMS), and has no effect on the poly(vinylferrocenium triflate) (PVTF) block. After extraction of un-cross-linked chains, the PaMS−I gels comprise solvent-filled, open channels inside a swollen PI network, while the swollen PVFT−I gels comprise channels of solvated PVFT chains inside a swollen PI network. The dependence of the structure, composition, and cross-linking density of the swollen microphases on radiation dose is determined by combining small-angle neutron scattering experiments with conventional gel characterization methods.

Introduction

Block copolymers provide a versatile platform for creating soft nanostructured materials with a wide variety of morphologies. These materials can be used in applications as diverse as flash memory and membranes.[1−4] Many of these applications require chemical or physical modification of the copolymers by processes such as cross-linking and chain scission. While the characterization of such materials in the dry state is relatively straightforward using standard techniques based on microscopy and scattering, characterization of swollen cross-linked block polymers is more difficult. The reason is that the partitioning of solvent between the polymer phases will, in general, be nonuniform. This is particularly true if one of the microphases is cross-linked and the other is not and if the solvent exhibits a different affinity for each of the blocks. Thus, the structure and microphase compositions of solvated block copolymer gels cannot be determined using information exclusively garnered from the dry state of the polymer and conventional methods of gel characterization such as swelling experiments. We show here that the desired information can be obtained from small-angle neutron scattering (SANS), which has been used previously to characterize swollen homopolymer gels[5,6] as well as solvated (un-cross-linked) block copolymers.[7−9] This effort is motivated by our recent investigations of electron-beam-treated diblock copolymers to create soft microporous materials that may be used as adsorbents or catalysts.[10]

Our work is focused on the characterization of two diblock copolymers exposed to electron beam (e-beam) radiation. The use of electron beam exposure is attractive as it offers uniform, room temperature cross-linking of the block copolymers without loss of microstructure.[11−14] The first polymer is poly(α-methylstyrene-*block*-isoprene) (PaMS−I). The polyisoprene (PI) microphase of this copolymer is cross-linked by exposure to the e-beam radiation; however, e-beam exposure depolymerizes the poly(α-methylstyrene) (PaMS) microphase, which can then be solvent extracted to produce a microporous, cross-linked solid. The second polymer is poly(vinylferrocenium triflate-*block*-isoprene) (PVFT−I). In this case, e-beam exposure causes cross-linking of the PI microphase but leaves the poly(vinylferrocenium triflate) (PVFT) microphase unaffected. Swelling of the exposed PVFT−I gel results in an active catalyst for a variety of chemical reactions. Our experiments provide quantitative answers to the following questions: (1) To what degree are the microphases cross-linked or degraded by the radiation? (2) How does the solvent partition in these microphases? (3) How does the swelling of cross-linked microphases differ from that of macroscopic cross-linked samples?

Experimental Methods

Poly(α-methylstyrene-*block*-isoprene) (PaMS−I) and poly(vinylferrocene-*block*-isoprene) (PVF−I) copolymers were synthesized by sequential anionic polymerization using THF as a solvent and *sec*-butyllithium as an initiator.[15,16] The PVF copolymer was oxidized using silver triflate in a benzene/methanol mixture to obtain a poly(vinylferrocenium triflate-*block*-isoprene) (PVFT−I) iron containing copolymer as described in ref 10. 90% of the ferrocene sites were oxidized to ferrocenium triflate. The chemical structures of both polymers are shown in Figure 1.

The copolymers were characterized by gel permeation chromatography (GPC) and proton NMR (H NMR) spectroscopy as described in ref 17. The polydispersity index of the PaMS−I copolymer was 1.02, and the molecular weights of the poly(α-methylstyrene) (PaMS) and polyisoprene (PI) (71% 3,4 addition) were 7.0 and 24.6 kg/mol, with the PaMS volume fraction of 0.20. The polydispersity index of the PVF−I copolymer was 1.11, and the molecular weights of the PVF and PI (75% 3,4 addition) were 3.7 and 8.3 kg/mol. Since the extent of oxidation is 90%, the molecular weight of the PVFT block in the PVFT−I copolymer is 6.0 kg/mol, and the volume fraction of poly(vinylferrocenium triflate) is 0.30.

Both polymers were freeze-dried from a benzene solution, and the resulting powder was pressed into discs with 5 mm diameter

* Corresponding authors. E-mail: nbalsara@berkeley.edu and alexbell@berkeley.edu.
[†] University of California, Berkeley.
[‡] Materials Sciences Division, Lawrence Berkeley National Laboratory.
[§] Environmental Energy Technologies Division, Lawrence Berkeley National Laboratory.
[⊥] Chemical Sciences Division, Lawrence Berkeley National Laboratory.
[#] Tyco Electronics Corporation.

10.1021/ma0629485 CCC: $37.00
Published on Web 06/15/2007

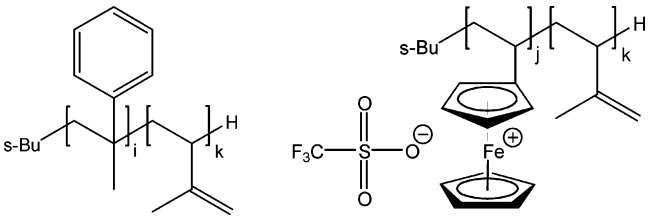

Figure 1. Structures of the block copolymers used in this study. Poly(α-methylstyrene-*block*-isoprene) (PaMS−I) is shown on the left, followed by poly(vinylferrocenium triflate-*block*-isoprene) (PVFT−I).

and 0.5 mm thickness. The samples were then irradiated by an e-beam to cross-link the PI chains and depolymerize the PaMS chains using facilities at Tyco Electronics in Menlo Park, CA. The samples were irradiated by a 3 MeV beam source using a series of ∼0.9 s exposures for total exposures of 40, 70, and 100 Mrad doses. The beam dose per exposure was 2.7 Mrad, and the time between successive exposures was 20 min. The beam dose was confirmed by a dosimeter that was exposed with the samples. The use of the e-beam facility was crucial, as all attempts to use peroxides to cross-link the PI phase in the PVFT−I copolymers led to uncontrolled degradation of the PVFT block.

Dry polymer samples were examined by transmission electron microscopy (TEM) at the National Center for Electron Microscopy at Lawrence Berkeley National Laboratory (LBNL). PVFT−I and PaMS−I were cryomicrotomed at −100 °C to obtain thin sections (ca. 50 nm) using a RMC Boeckler PTXL ultramicrotome with a cryogenic attachment. Sections were collected on copper grids, and the PaMS−I samples were stained with osmium tetroxide for enhancing electron contrast between the microphases. Staining of the PVFT−I copolymer was not required due to the natural electron contrast between the iron-containing and the organic blocks. The sections were then placed in a JEOL 200CX electron microscope and imaged in the dry state.

The gels were swollen and characterized gravimetrically. The cross-linked discs (ca. 12 mg) were placed in ∼2 mL of a good solvent: cyclohexane for PaMS−I and 1,2-dichlorobenzene for PVFT−I. The gels were allowed to equilibrate for 24 h in the solvent. The supernatant was removed and reserved for later characterization. The ratio of the mass of the resultant swollen gel to that of the dry sample gives the swelling ratio, SR. The swollen gel materials were then dried to constant weight in a vacuum oven for a period of ∼1 week at 190 °C. A constant weight condition could not be achieved at lower temperatures. The ratio of the mass of the dried gel material to that of the original dry sample prior to swelling gives the gel fraction, GF. The supernatant from the swelling experiments was dried to constant weight under vacuum at ambient temperatures to isolate the chains not attached to the network. These chains were then dissolved in deuterated chloroform ($CDCl_3$) and analyzed by H NMR spectroscopy. Peaks corresponding to chemical moieties present on the chains were integrated to determine the composition of the chains extracted from the network.

SANS sample cells were prepared by first gluing one quartz window to an anodized aluminum spacer with Devcon two-part, 5 min epoxy. The spacer inner diameter was 7.5−10 mm, depending on the anticipated degree of swelling of the gel, and the spacer thickness was about 1 mm. A series of samples were created by swelling each irradiated sample in mixtures of hydrogenated and deuterated solvents. The neutron scattering length densities (SLD) of the components, given in Tables 1 and 2, were calculated using the scattering lengths of the atoms in each component and the (mass) densities of each component.[18] Another quartz disc was then glued and clamped to the assembly to make an airtight seal. The thicknesses of the gels, quartz windows, and total assembly were measured in order to determine the thickness of the scattering sample. Because ferrocenium triflate degrades in air, all of the experiments on the PVFT−I samples were done either in an argon glovebox or in cells that were sealed in the glovebox. SANS samples are labeled according to both radiation dose and volume fraction of deuterated swelling solvent. Thus, PaMS−I-40(0.33) implies that the PaMS−I was cross-linked with 40 Mrad exposure and swollen in a cyclohexane/cyclohexane-d_{12} mixture with 33 vol % cyclohexane-d_{12}.

Table 1. Neutron Scattering Length Densities for the Polymers and Solvents Used in the Swelling of the PaMS−I Materials

species	scattering length density ($\times 10^4$ nm^{-2})
poly(α-methylstyrene) (PaMS)	1.18
polyisoprene (PI)	0.256
cyclohexane	−0.278
cyclohexane-d_{12}	5.84

Table 2. Neutron Scattering Length Densities for the Polymers and Solvents Used in the Swelling of the PVFT−I Materials

species	scattering length density ($\times 10^4$ nm^{-2})
poly(vinylferrocenium triflate) (PVFT)	2.24
polyisoprene (PI)	0.256
1,2-dichlorobenzene	1.97
1,2-dichlorobenzene-d_{12}	4.58

SANS experiments were conducted on the NG7 beamline at the National Institute of Standards and Technology in Gaithersburg, MD. SANS data were gathered at room temperature for the PaMS−I samples and 50 °C for the PVFT−I samples. Two-dimensional SANS patterns were measured as a function of scattering angle with the neutron wavelength, $\lambda = 0.6$ nm and wavelength spread $\Delta\lambda/\lambda = 0.1$. The raw data were azimuthally symmetric and converted to absolute coherent scattering intensity, I, as a function of the magnitude of the scattering vector q, $q = 4\pi \sin(\theta/2)/\lambda$, where θ is the scattering angle and λ is the wavelength of the incident beam. Corrections for detector sensitivity, background, empty cell, and incoherent scattering were made using procedures given in ref 19.

Data Analysis

We now develop the equations that are necessary to determine the size and composition of the swollen block copolymer microphases. Here, superscript "i" indicates properties of the initial polymer prior to swelling, superscript "f" indicates properties of the final swollen gel after extraction of the free chains, and superscript "s" indicates properties of the supernatant during the swelling/extraction experiment. We consider an irradiated A−B copolymer where the B-block is selectively cross-linked. The A-rich microphase is labeled α, and the B-rich microphase is labeled β. The subscripts "poly" and "solv" refer to the polymer and solvent, respectively. A schematic of the swelling process as well as all of the relevant volumes and densities is defined in Figure 2. Here m is an index referring to either α or β microphase, while M refers to the polymer identity and can be either A or B. Relevant volume fractions for the system can also be defined:

$$\phi^{\alpha} = \frac{V^{f,\alpha}_{poly} + V^{f,\alpha}_{solv}}{V^{f,\alpha}_{poly} + V^{f,\alpha}_{solv} + V^{f,\beta}_{poly} + V^{f,\beta}_{solv}} = 1 - \phi^{\beta} \qquad (1)$$

ϕ^{α} is the volume fraction of the α-microphase. Note that ϕ^{α} and ϕ^{β} sum to unity.

$$\phi^{m}_{poly} = \frac{V^{f,m}_{poly}}{V^{f,m}_{poly} + V^{f,m}_{solv}} = 1 - \phi^{m}_{solv} \qquad (2)$$

ϕ^{m}_{poly} is the volume fraction of polymer within the m microphase of the gel. As the microphase consists only of polymer and solvent, ϕ^{m}_{poly} and ϕ^{m}_{solv} sum to unity.

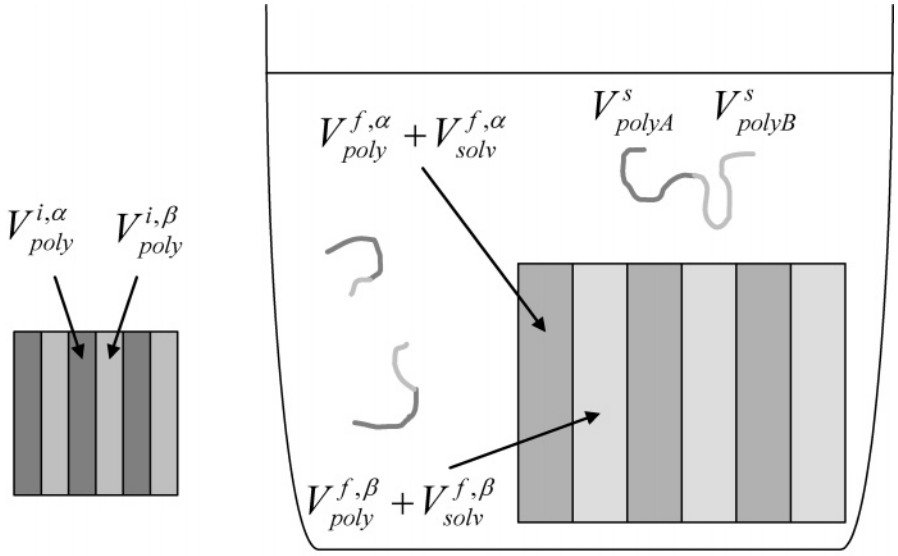

$V^{i,m}_{poly}$	Volume of polymer in the m phase in the dry gel prior to swelling.
V^{s}_{polyM}	Volume of polymer of type M extracted to the supernatant.
$V^{f,m}_{poly}$	Volume of polymer in the m phase of the gel after swelling.
$V^{f,m}_{solv}$	Volume of solvent in the m phase of the gel after swelling.
ρ_{polyM}	Density of polymer of type M.
ρ_{solv}	Density of the swelling solvent.

Figure 2. Schematic for the swelling process of the gels in this study showing a gel prior to swelling (left) and after swelling (right). Note that actual swollen gels do not consist of a single domain. The chains in the supernatant can consist of whole chains (PaMS−I and PVFT−I) or chain fragments (PaMS−I). The relevant volumes and densities are also shown.

To obtain tractable solutions to the governing equations, we assume that there is no intermixing between the A and B blocks, in either the neat or swollen states, and neglect volume changes of mixing. Simple mass balances can be written to obtain the following expressions for the swelling ratio (SR) and the gel fraction (GF):

$$\frac{\text{mass of swollen gel}}{\text{mass of dry gel}} = \text{SR} = \frac{\rho_{\text{polyA}}V^{\text{f},\alpha}_{\text{poly}} + \rho_{\text{polyB}}V^{\text{f},\beta}_{\text{poly}} + \rho_{\text{solv}}(V^{\text{f},\alpha}_{\text{solv}} + V^{\text{f},\beta}_{\text{solv}})}{\rho_{\text{polyA}}V^{\text{f},\alpha}_{\text{poly}} + \rho_{\text{polyB}}V^{\text{f},\beta}_{\text{poly}}} \quad (3)$$

and

$$\frac{\text{mass of polymer in gel after extraction of free chains}}{\text{mass of polymer in gel prior to extraction of free chains}} = \text{GF} = \frac{\rho_{\text{polyA}}V^{\text{f},\alpha}_{\text{poly}} + \rho_{\text{polyB}}V^{\text{f},\beta}_{\text{poly}}}{\rho_{\text{polyA}}V^{\text{i},\alpha}_{\text{poly}} + \rho_{\text{polyB}}V^{\text{i},\beta}_{\text{poly}}} \quad (4)$$

where ρ is density and V is volume as defined in Figure 2.

The molar ratio of the supernatant chains determined by NMR, R, is given by

$$\frac{\text{number of A repeat units in supernatant}}{\text{number of B repeat units in supernatant}} = R = \frac{\rho_{\text{polyA}}V^{\text{s}}_{\text{polyA}}/\text{MW}_{\text{polyA}}}{\rho_{\text{polyB}}V^{\text{s}}_{\text{polyB}}/\text{MW}_{\text{polyB}}} \quad (5)$$

where MW is the monomer molecular weight of each species. A is the un-cross-linked block (PaMS or PVFT), and B is the cross-linked isoprene block. In the case of PVFT−I, the extracted polymer is either individual PVFT−I chains or clusters of PVFT−I chains. The A-to-B ratio inside the gel is thus identical to that of the original A−B copolymer. In the case of PaMS−I, however, the degraded fragments of the PaMS chains are dissolved along with the unconnected and undegraded copolymer chains, and thus the A-to-B ratio inside the gel will be different than that in the original A−B copolymer.

Two relationships between the volumes contained in each microphase can be written as follows:

$$V^{\text{i},m}_{\text{poly}} = V^{\text{f},m}_{\text{poly}} + V^{\text{s}}_{\text{polyM}} \qquad m = \alpha, \beta; M = A, B \quad (6, 7)$$

We also know the composition of our system initially, so the quantities $V^{\text{i},\alpha}_{\text{poly}}$ and $V^{\text{i},\beta}_{\text{poly}}$ are known constants.

Equations 4−7 can be solved for the four unknowns ($V^{\text{f},\alpha}_{\text{poly}}$, $V^{\text{f},\beta}_{\text{poly}}$, $V^{\text{s}}_{\text{polyA}}$, $V^{\text{s}}_{\text{polyB}}$). However, the two relevant quantities in the experiment are the volumes of polymer in the gel after swelling:

Equation 3 is thus far unused and can be rewritten by combining with eq 4 to yield a relationship between the final amount of

$$V^{\text{f},\alpha}_{\text{poly}} = \frac{\rho_{\text{polyA}}V^{\text{i},\alpha}_{\text{poly}}(\text{MW}_{\text{polyB}} + \text{GF}\cdot R\cdot\text{MW}_{\text{polyA}}) + \rho_{\text{polyB}}V^{\text{i},\beta}_{\text{poly}}(\text{GF} - 1)\text{MW}_{\text{polyA}}}{\rho_{\text{polyA}}(R\cdot\text{MW}_{\text{polyA}} + \text{MW}_{\text{polyB}})} \quad (8)$$

$$V^{\text{f},\beta}_{\text{poly}} = \frac{\rho_{\text{polyA}}V^{\text{i},\alpha}_{\text{poly}}(GF - 1)\text{MW}_{\text{polyB}} + \rho_{\text{polyB}}V^{\text{i},\beta}_{\text{poly}}(\text{GF}\cdot\text{MW}_{\text{polyB}} + R\cdot\text{MW}_{\text{polyA}})}{\rho_{\text{polyB}}(R\cdot\text{MW}_{\text{polyA}} + \text{MW}_{\text{polyB}})} \quad (9)$$

solvent in each microphase, known initial volumes ($V^{i,\alpha}_{poly}$, $V^{i,\beta}_{poly}$), and other known quantities.

$$V^{f,\alpha}_{solv} + V^{f,\beta}_{solv} = \frac{GF}{\rho_{solv}}(\rho_{polyA}V^{i,\alpha}_{poly} + \rho_{polyB}V^{i,\beta}_{poly})(SR - 1) \quad (10)$$

Thus, the total amount of solvent in the gel is known, but the amount partitioned into each microphase is yet to be determined. We use SANS data to estimate solvent partitioning. The scattering intensity at the peak increases as the deuterium content of the swelling solvent is increased. This is due to increasing contrast between the microphases, as expected from the scattering length densities given in Tables 1 and 2.

Analysis of this change in intensity with contrast allows the determination of the solvent partitioning in the gel by using eqs 8−10. We assume that the structure of the gels is not affected by solvent deuteration. In this case the intensity, I, is proportional to the square of the difference between the scattering length densities of microphases α and β[20]

$$I \propto (\varsigma^{\alpha} - \varsigma^{\beta})^2 \equiv c \quad (11)$$

where c represents the scattering contrast of the system and ς^m ($m = \alpha, \beta$), the scattering length density of each microphase, is given in terms of the scattering length densities of the pure components ς^m_{polyM} and ς^m_{solv}.

$$\varsigma^m = \left(\frac{V^{f,m}_{poly}}{V^{f,m}_{poly} + V^{f,m}_{solv}}\right)\varsigma^m_{polyM} + \left(\frac{V^{f,m}_{solv}}{V^{f,m}_{poly} + V^{f,m}_{solv}}\right)\varsigma^m_{solv} = \phi^m_{poly}\varsigma^m_{polyM} + \phi^m_{solv}\varsigma^m_{solv} \quad (12)$$

The scattering contrast is unknown because the partitioning of the solvent in the microphases is unknown. We use an iterative procedure to determine the contrast. We assume a value for $V^{f,\alpha}_{solv}$, compute $V^{f,\beta}_{solv}$ using eq 10, and then compute the contrast (c) for each sample using eqs 11 and 12. We then perform a least-squares linear fit of the SANS intensity (I) vs c and the value of $V^{f,\alpha}_{solv}$ that provides the best fit is taken as the solvent content of the α-microphase. While eq 11 applies at any value of q, we use the peak intensity, I_{peak}, as the signal-to-noise ratio is highest at this point.

The correlation coefficient (r value) is defined as

$$r = \frac{\sigma_{cI}}{\sigma_c\sigma_I} = \frac{\sum(c_j - \bar{c})(I_j - \bar{I})}{\sqrt{\sum(c_j - \bar{c})^2\sum(I_j - \bar{I})^2}} \quad (13)$$

Here σ_{cI} is the covariance of a data set, σ_c and σ_I are the standard deviations of the data sets, I is intensity, and c is contrast. The summations include all data points, and the overbars denote the mean of the set. By maximizing r in eq 13 subject to the constraint of eq 10, we arrive at the contrast of each sample, which, in turn, enables determination of all of the volumes in the system defined in Figure 2. Our method for analyzing the SANS data is not unique. Other methods (e.g., extracting information based on the slopes and intercepts of linear fits of $I^{1/2}$ vs ς^m_{solv} data) give results that are qualitatively similar to those presented here.

Results and Discussion

In Figure 3 we show a typical micrograph of PVFT−I where a lamellar morphology is observed. TEM was also performed on an irradiated sample of PVFT−I. No change in microstructure was observed. The micrograph of unirradiated PaMS−I shown in Figure 4 indicates the presence of a cylindrical morphology.

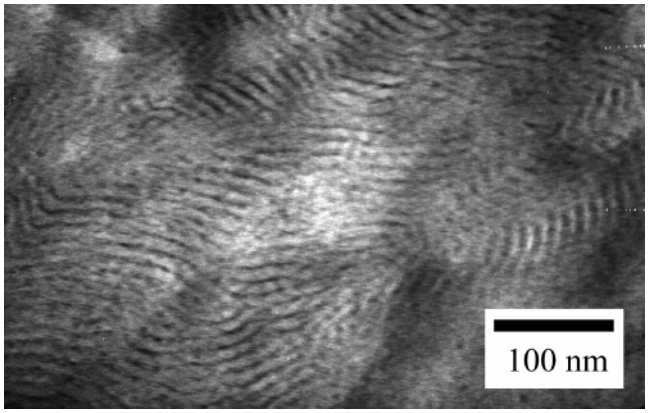

Figure 3. Transmission electron micrograph of the unirradiated poly(vinylferrocenium triflate-*block*-isoprene) copolymer showing a lamellar morphology. The poly(vinylferrocenium triflate) block appears dark, and the polyisoprene block appears light.

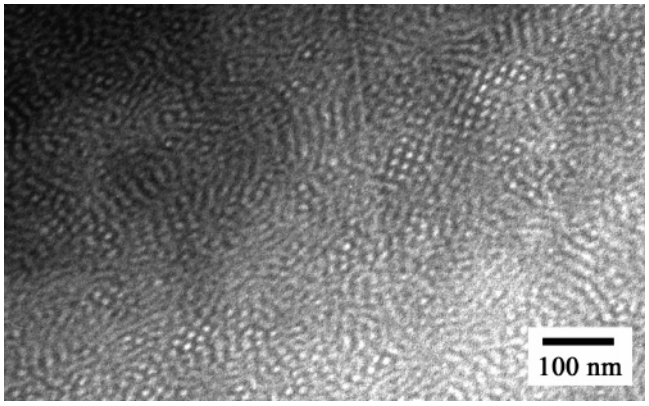

Figure 4. Transmission electron micrograph of the unirradiated poly(α-methylstyrene-*block*-isoprene) copolymer showing a periodic hexagonal morphology. The polyisoprene block appears dark due to staining with osmium tetroxide.

Table 3. Results of Swelling and Drying Experiments[a]

sample	swelling ratio (SR)	gel fraction (GF)
PaMS−I-40	11.5	0.914
PaMS−I-70	7.1	0.947
PaMS−I-100	6.2	0.964
PVFT−I-40	13.8	0.783
PVFT−I-70	8.6	0.901
PVFT−I-100	6.6	0.983

[a] Estimated errors in SR and GF are about 5%.

The swelling ratio and gel fraction data obtained from all samples are given in Table 3. It is instructive to compare our findings with the well-studied case of homopolymer gels, where increasing the cross-linking density leads to a decrease in the swelling ratio (SR) and an increase in the gel fraction (GF).[21] We expect qualitatively similar behavior in the PVFT−I system due to the absence of chain degradation, and this is confirmed in Table 3. In the case of PaMS−I, however, increased radiation dose leads to increased PaMS chain degradation. The voids left behind by the degraded and extracted chains could, in principle, provide more open space in the gel in which the solvent could reside. This could lead to an increase in SR with increasing dose. The data in Table 3 show the opposite trend. It is evident that the swelling and drying data of PaMS−I gels are dominated by the increase in cross-linking density of the PI block with increasing dose.

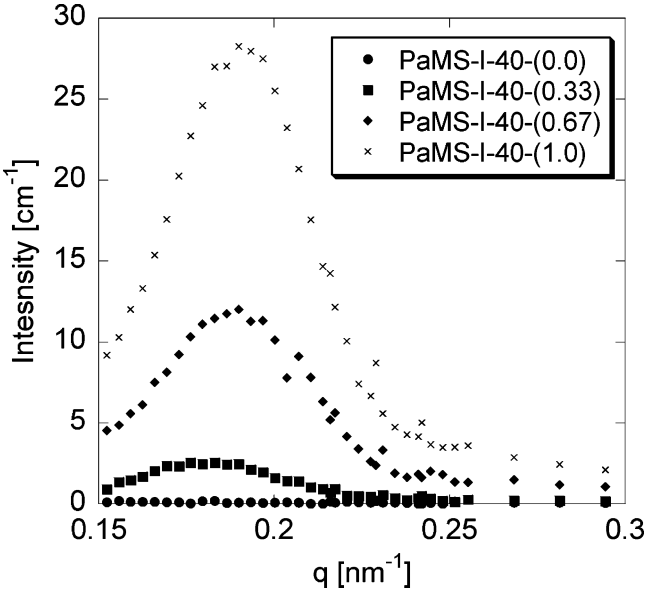

Figure 5. SANS intensity, *I*, vs scattering vector, *q*, from a series of PaMS−I-40 gels swollen in solvents with different levels of deuterium. The number in the parentheses is the volume fraction of cyclohexane-d_{12} in the swelling solvent.

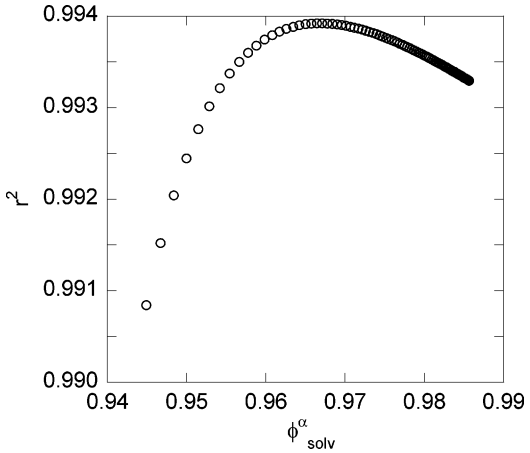

Figure 6. Plot of the square of the correlation coefficient vs the trial values of the volume fraction of solvent in the α-microphase for PaMS−I-40.

Data from the SANS profiles from selected PaMS−I-40 samples are shown in Figure 5. All of the samples contained a primary scattering peak at approximately $q = 0.2$ nm^{-1}. No higher order peaks were observed in the scattering from any of the gel samples. One might expect a decrease in long-range order in swollen samples due to the isotropic nature of the swelling process and the anisotropic nature of the ordered microphases. However, no higher order scattering peaks were seen in the dry PaMS−I SANS data, despite evidence of an ordered sample in the TEM data (Figure 4). This is probably due to the relatively low resolution of the SANS instrument. The scattering data from the series of gels for PaMS−I-70 and PaMS−I-100 are qualitatively similar to the PaMS−I-40 data shown in Figure 5. The iterative SANS analysis procedure described in the data analysis section was applied to all of the PaMS−I samples. The square of the correlation coefficient, *r*, as a function of trial values of ϕ^{α}_{solv} in the PaMS−I-40 gel is shown in Figure 6. The location of the maximum in Figure 6 gives the composition of the gel in the α-microphase and the scattering contrast, *c*. The *r* vs ϕ^{α}_{solv} curves obtained from the other gels were similar to those shown in Figure 6. Plots of

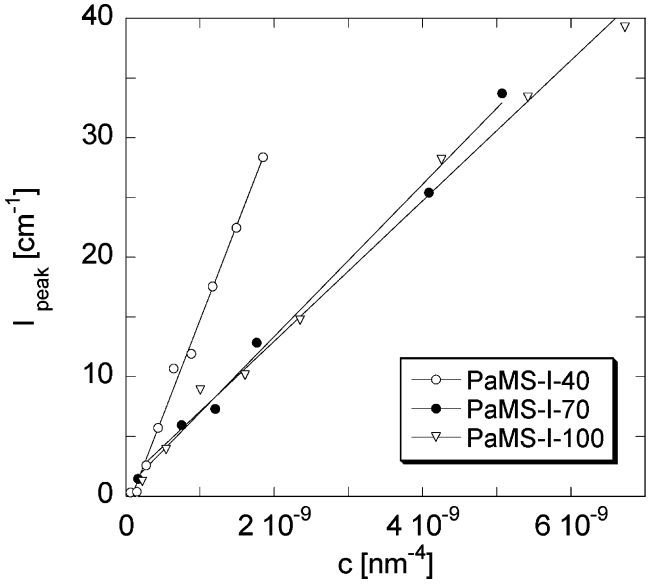

Figure 7. SANS peak intensity vs the contrast factor for PaMS−I gels. The line represents the result of the fitting procedure described in the Data Analysis section.

I_{peak} vs *c* thus obtained from all of the PaMS−I gels are given in Figure 7, and the gel characteristics determined from the analysis procedure are summarized in Table 4. The volume fraction of the α-microphase (ϕ^{α}) is ∼0.4 for all samples PaMS−I-40, PaMS−I-70, and PaMS−I-100. This indicates that the decreased swelling of the β-microphase with increasing radiation is balanced by the size reduction of the α-microphase due to chain scission and subsequent loss of the unattached chains. In the case of block copolymer melts, as well as block copolymers dissolved in a common solvent, one obtains a lamellar morphology when the volume fraction of one of the microphases is 0.40.[22−24] We assume that this is true for our system and compute the lamellar thicknesses from the position of the SANS peak. The results thus obtained are given in Table 4. The assumed morphology in the swollen state is different from the cylindrical morphology seen in the neat diblock copolymer. While we do not have conclusive proof regarding the existence of a lamellar morphology in the gels due to the absence of higher order peaks in the SANS data, many of our conclusions (e.g., the compositions of the microphases) are not dependent on this assumption. If we assume that we have a cylindrical morphology, then the radii of the cylinders are 13.1, 11.6, and 11.2 nm for the PaMS−I-40, PaMS−I-70, and PaMS−I-100 gels, respectively.

It is evident from Table 4 that the α-microphase in the swollen PaMS−I gels contains very little polymer (between 3 and 7%). This indicates the e-beam exposure was effective in depolymerization of the PaMS block. We thus have a gel with pores that are almost entirely filled with solvent. The presence of these pores could be exploited in applications such as catalysis and separation. The NMR measurements indicated that increasing the radiation dose led to increased molar ratios of PaMS chains in the supernatant. The molar ratios of the monomers in the supernatant, ($R = N_{PaMS}/N_{PI}$) for the PaMS−I gels were determined to be 0.67, 1.06, and 1.22 for the PaMS−I-40, PaMS−I-70, and PaMS−I-100, respectively, indicating increasing chain scission with increasing radiation dose. The SANS analysis indicates that the concentration of PaMS in the α-microphase increases with increasing radiation dose, as shown in Table 4. This apparent contradiction is due to the tightening of the PI network with increasing radiation dose. The data in

Table 4. PaMS−I Gel Characterization Results[a]

sample	ϕ^{α}	ϕ^{α}_{sol}	ϕ^{α}_{PaMS}	ϕ^{β}_{sol}	ϕ^{β}_{PI}	q_{peak} [nm^{-1}]	d [nm]	d_{α} [nm]	M_c [kg/mol]
PaMS−I-40	0.41	0.97	0.03	0.90	0.10	0.185	34.0	13.8	8.3
PaMS−I-70	0.40	0.94	0.06	0.83	0.17	0.208	30.1	12.1	5.1
PaMS−I-100	0.41	0.93	0.07	0.80	0.20	0.217	28.9	11.7	4.1

[a] The volume fraction of the α-microphase is shown in column 2. Phase compositions are shown in columns 3−6. q_{peak} from the primary peak in the scattering experiment and corresponding d ($d = 2\pi/q_{peak}$) are located in columns 7 and 8. The calculated domain sizes for a lamellar network, d_{α}, representing the thickness of the α-microphase in a lamellar system is given in column 9. The molecular weight between cross-links in the polyisoprene microphase is shown in column 10.

Table 4 show that d_{α}, the thickness of the α lamellae, decreases with increasing radiation dose due to this tightening. Network tightening outweighs the slight increase in PaMS chain scission at higher dose, giving a higher PaMS concentration in the pores.

For affinely deformed swollen homopolymer networks, the relationship between the average molecular weight between cross-links (M_c) and the properties of the swollen gel[25−28] is given by

$$M_c = \frac{v_{sol}\rho_{poly}\left(\frac{\phi_{poly}}{2} - \phi_{poly}^{1/3}\right)}{\ln(1-\phi_{poly}) + \phi_{poly} + \chi_{SP}\phi_{poly}^{2} + \frac{v_{sol}\rho_{poly}}{2M_n}(\phi_{poly} - 4\phi_{poly}^{1/3})} \quad (14)$$

Here, v_{sol} is the solvent molar volume, ρ_{poly} is the dry polymer density, χ_{SP} is the solvent−polymer interaction parameter, M_n is the number-average molecular weight of the polymer participating in the network, and ϕ_{poly} is the polymer volume fraction at swelling equilibrium. Equation 14 was used to determine the swelling in the PI microphase of the PaMS−I gels by setting $\phi_{poly} = \phi^{\beta}_{PI}$, $\rho_{poly} = 0.890$ g/cm^3 (density of dry PI at 25 °C), and $v_{sol} = 108$ cm^3/mol and then computing M_c for each gel. For simplicity, we present results obtained with $\chi_{SP} = 0.4$.[29] The resulting values of M_c are given in Table 4. Since there is some uncertainty in the value of χ_{SP}, we calculated M_c for χ_{SP} values of 0.35 and 0.45. Although our choice of χ_{SP} affects the numerical value of M_c, it has no qualitative effect on our analysis. For example, M_c values for PaMS−I-70 with χ_{SP} values of 0.35 and 0.45 are 4.4 and 6.2 kg/mol, respectively. M_c values of other samples were either equally or less sensitive to variations in χ_{SP}. In previous studies[30,31] eq 14 was applied to the swollen block copolymer data, ignoring the presence of microstructure to estimate the molecular weight between cross-links from swelling of block copolymers. If we were to use eq 14 directly on swelling ratios measured for the entire gel, we would obtain M_c values of 9.5, 7.1, and 6.2 kg/mol for the PaMS−I-40, PaMS−I-70, and PaMS−I-100 gels, respectively ($\chi_{SP} = 0.4$). We see that the present analysis gives significantly lower values for M_c, and the deviations increase with increasing dose (see Table 4). These deviations suggest that the un-cross-linked PaMS block plays an increasingly important role in the swelling of cross-linked PaMS−I samples as radiation dose is increased. We note that while the present method for determining M_c is more complete than that in previous literature, there is considerable room for improvement. For example, the application of more complete swelling theories that account for the specific geometry of the microphases and effects such as nonaffine deformation will lead to more precise estimates of M_c.

Selected SANS profiles from the PVFT−I-40 gels are shown in Figure 8. We see the presence of a single scattering peak located at $q = 0.35$ nm^{-1} that increases in intensity as the deuterium content of the solvent is increased. The PVFT−I gels are, however, characterized by a significant enhancement of low-q scattering, a feature that was not present in the PaMS−I gels (compare Figures 5 and 8). This feature is attributed to the presence of electrostatic charge on the vinyl ferrocenium triflate moieties in PVFT−I gels (see Figure 1). Similar low-q upturns have been seen in other charged polymer solutions[32−34] and dry block copolymers containing ferrocenium.[35] The origin of this feature is a matter of considerable debate and not discussed here. Following ref 35, we assume the SANS profiles in the vicinity of q_{peak} to be given by the sum of a Gaussian peak and an exponentially decaying background. The peak height thus obtained, I_{peak}, was used in the SANS data analysis described above. The scattering data from the series of gels for PVFT−I-70 and PVFT−I-100 are qualitatively similar to the data shown in Figure 8, and the same methodology was used to analyze the SANS data. Plots of I_{peak} vs c thus obtained for PVFT−I-40, PVFT−I-70, and PVFT−I-100 are shown in Figure 9, and the gel characteristics determined from the analysis are summarized in Table 5.

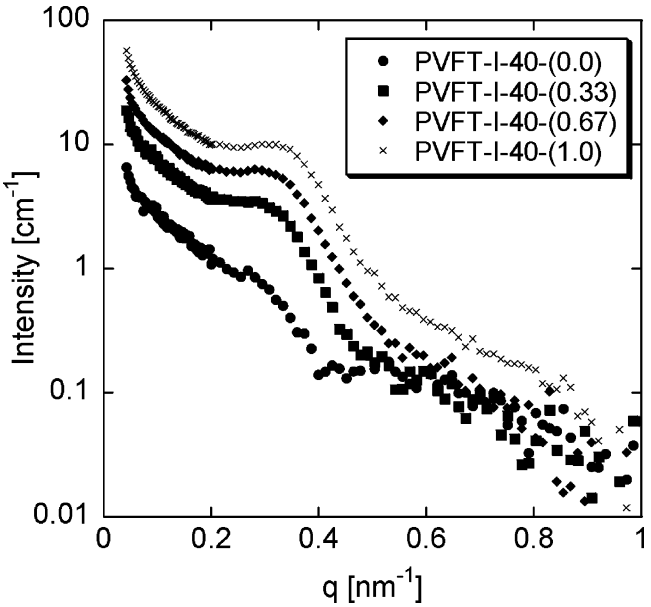

Figure 8. SANS intensity, I, vs scattering vector, q, from a series of PVFT−I-40 gels swollen in solvents with different levels of deuterium. The number in the parentheses is the volume fraction of 1,2-dichlorobenzene-d_4 in the swelling solvent.

The volume fraction of the α-microphase (containing PVFT) increases from 0.50 to 0.63 with increasing dosage (Table 5). In this range of volume fractions, we expect to obtain a lamellar morphology, which is identical to that obtained in the bulk. The lamellar thicknesses, d_{α}, based on the location of the SANS peaks are given in Table 5. A modest increase in d_{α} from 8.2 to 9.7 nm is seen with increasing dose. The stretching of the PVFT chains, which are not degraded by the e-beam exposure, is thus seen to increase slightly as the cross-linking density of the PI microphase is increased.

Table 5. PVFT−I Gel Characterization Results[a]

sample	ϕ^{α}	ϕ^{α}_{sol}	ϕ^{α}_{PVFT}	ϕ^{β}_{sol}	ϕ^{β}_{PI}	q_{peak} [nm^{-1}]	d [nm]	d_{α} [nm]	M_c [kg/mol]
PVFT−I-40	0.40	0.93	0.07	0.90	0.10	0.304	20.7	8.2	3.5
PVFT−I-70	0.56	0.92	0.08	0.78	0.22	0.363	17.3	9.7	2.2
PVFT−I-100	0.63	0.91	0.09	0.67	0.33	0.406	15.5	9.7	1.3

[a] The volume fraction of the α-microphase is shown in column 2. Phase compositions are shown in columns 3−6. q_{peak} from the primary peak in the scattering experiment and corresponding d ($d = 2\pi/q_{peak}$) are located in columns 7 and 8. The calculated domain sizes for a lamellar network, d_{α}, representing the thickness of the α-microphase in a lamellar system is given in column 9. The molecular weight between cross-links in the polyisoprene microphase is shown in column 10.

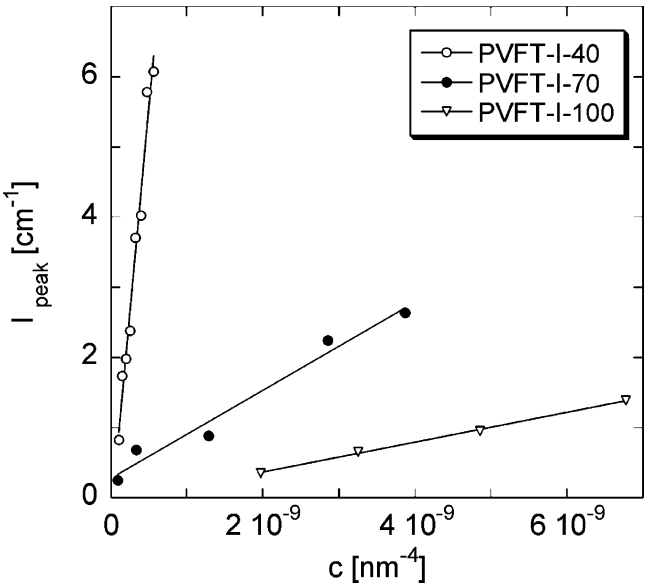

Figure 9. SANS peak intensity vs the contrast factor for PVFT−I gels. The line represents the result of the fitting procedure described in the Data Analysis section.

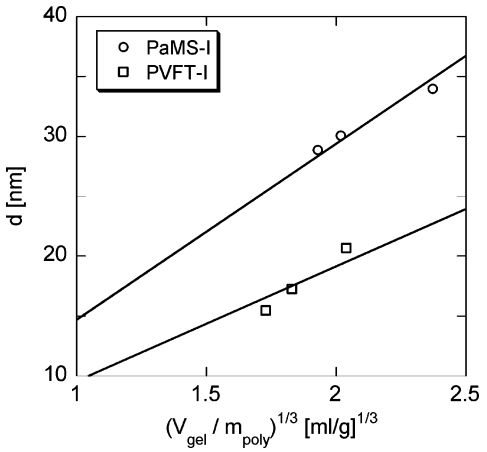

Figure 10. Characteristic domain spacing (d) as determined from SANS vs specific volume of the swollen gel. Both parameters decrease monotonically with radiation dose (40, 70, and 100 Mrad). The uncertainty in the measurement of gel volume is about 5%. The lines are least-squares fits, constrained to go through the origin.

The microphase sizes are related to the composition within the phases. Mass balances dictate that changes in the solvent partitioning change both the relative sizes of the microphases and the composition within the microphases. The PVFT−I gels mimicked the composition behavior of PaMS−I in the PI microphase. As the dosage increased, more cross-links were made in the PI microphase, and this led to a decrease in solvent uptake, as shown in Table 5.

We compute the molecular weight between cross-links by applying the affine network model to the β-microphase swelling characteristics in the PVFT−I gels using the same computation method as that used to analyze the PaMS−I gels with $\chi_{SP} = 0.4$, $\rho_{poly} = 0.890$ g/cm^3, and $\upsilon_{sol} = 113$ cm^3/mol. The resulting M_c values are given in Table 5. Applying eq 14 to the macroscopic swelling data gives M_c values of 3.5, 2.8, and 2.4 kg/mol, for PVFT−I-40, PVFT−I-70, and PVFT−I-100, respectively. The discrepancy between M_c values obtained by bulk and microscopic analysis is smaller in the PVTF−I case than that in the PaMS−I case. This is probably because of the large porosity in PaMS−I gels due to chain scission.

In Figure 10, we show the relationship between size of the swollen microphases as measured by SANS and the macroscopic sample size. We see that the d-spacing ($d = 2\pi/q_{peak}$) is proportional to the 1/3 power of the swollen gel volume per gram of polymer. This indicates that the swelling occurs isotropically and uniformly in our cross-linked block copolymers.

Conclusions

We have determined the structure and composition of microphases in swollen block copolymer gels obtained by selectively cross-linking one of the blocks. We studied gels obtained from poly(α-methylstyrene-*block*-isoprene) (PaMS−I) and poly(vinylferrocenium triflate-*block*-isoprene) (PVFT−I) copolymers wherein the PI block was cross-linked by e-beam irradiation. The e-beam irradiation degrades the PaMS block to create open channels but has no effect on the PVFT block. A combination of SANS and conventional gel characterization methods was used to determine all of the important characteristics of the gels. We demonstrate that the nature of the microphases in the two systems is qualitatively different due to differences in the effect of the e-beam processing. The results of our analyses on the PaMS−I and PVFT−I systems are summarized in Tables 4 and 5, respectively, where we quantify the effect of radiation dose on (1) the extent of chain scission and cross-linking in each microphase due to radiation, (2) solvent partitioning between the cross-linked and non-cross-linked phases, and (3) the molecular weight between cross-links. We have thus answered all of the questions raised in the Introduction. This work lays the foundation for a systematic study of the relationship between morphology and catalytic activity in PVFT-containing block copolymer gels which is the subject of current studies.

Acknowledgment. Financial support for this work was provided by the National Science Foundation, CTS-0625785. The TEM facilities at the National Center for Electron Microscopy, Lawrence Berkeley National Laboratory, are supported by the Office of Basic Energy Sciences of the U.S. Department of Energy under Contract DE-AC03-76SF00098. The SANS facilities at NIST are supported in part by the National Science Foundation under Agreement DMR-0504122. Preliminary SANS experiments were conducted at the Intense Pulsed Neutron Source (IPNS) at Argonne National Laboratory with guidance from Dennis Wozniak and P. Thiyagarajan. The IPNS is

supported by the Department of Energy Office of Basic Energy Sciences, Contract W-31-109-ENG-38.

References and Notes

(1) Kim, S. O.; Solak, H. H.; Stoykovich, M. P.; Ferrier, N. J.; de Pablo, J. J.; Nealey, P. F. *Nature (London)* **2003**, *424*, 411−414.
(2) Guarini, K. W.; Black, C. T.; Zhang, Y.; Kim, H.; Sikorski, E. M.; Babich, I. V. *J. Vac. Sci. Technol. B* **2002**, *20*, 2788−2792.
(3) Lipic, P. M.; Bates, F. S.; Hillmyer, M. A. *J. Am. Chem. Soc.* **1998**, *120*, 8963−8970.
(4) Du, P.; Li, M. Q.; Douki, K.; Li, X. F.; Garcia, C. R. W.; Jain, A.; Smilgies, D. M.; Fetters, L. J.; Gruner, S. M.; Wiesner, U.; Ober, C. K. *Adv. Mater.* **2004**, *16*, 953−957.
(5) Benoit, H.; Decker, D.; Duplessix, R.; Picot, C.; Rempp, P. *J. Polym. Sci., Part B: Polym. Phys.* **1976**, *14*, 2119−2128.
(6) Bastide, J.; Duplessix, R.; Picot, C.; Candau, S. *Macromolecules* **1984**, *17*, 83−93.
(7) Castelletto, V.; Hamley, I. W.; Pedersen, J. S. *J. Chem. Phys.* **2002**, *117*, 8124−8129.
(8) Mortensen, K.; Almdal, K.; Kleppinger, R.; Mischenko, N.; Reynaers, H. *Physica B* **1997**, *241*, 1025−1028.
(9) Lodge, T. P.; Hamersky, M. W.; Hanley, K. J.; Huang, C. I. *Macromolecules* **1997**, *30*, 6139−6149.
(10) Durkee, D. A.; Eitouni, H. B.; Gomez, E. D.; Ellsworth, M. W.; Bell, A. T.; Balsara, N. P. *Adv. Mater.* **2005**, *17*, 2003−2006.
(11) Bly, J. H. *J. Ind. Irradiat. Technol.* **1983**, *1*, 51−75.
(12) Yunshu, X.; Siswono, H.; Fumio, Y.; Keizo, M. *J. Appl. Polym. Sci.* **1997**, *66*, 113−116.
(13) Grobler, J. H. A.; McGill, W. J. *J. Polym. Sci., Part B: Polym. Phys.* **1994**, *32*, 287−295.
(14) Chapiro, A. *Radiation Chemistry of Polymeric Systems*; Interscience Publishers: New York, 1962; Vol. XV.
(15) Fetters, L. J.; Morton, M. *Macromolecules* **1969**, *2*, 453−458.
(16) Nuyken, O.; Burkhardt, V.; Hubsch, C. *Macromol. Chem. Phys.* **1997**, *198*, 3353−3363.
(17) Reynolds, B. J.; Ruegg, M. L.; Balsara, N. P.; Radke, C. J.; Shaffer, T. D.; Lin, M. Y.; Shull, K. R.; Lohse, D. J. *Macromolecules* **2004**, *37*, 7401−7417.
(18) Roe, R. J. *Methods of X-Ray and Neutron Scattering in Polymer Science*; Oxford University Press: New York, 2000.
(19) Kline, S. *SANS Reduction Tutorial*; NIST Center for Neutron Research: Gaithersburg, MD, 1991.
(20) Higgins, J. S.; Benoit, H. C. *Polymers and Neutron Scattering*; Clarendon Press: Oxford, 1994.
(21) Treloar, L. R. G. *Physics of Rubber Elasticity*; Oxford University Press: Oxford, 1975.
(22) Bates, F. S.; Schulz, M. F.; Khandpur, A. K.; Forster, S.; Rosedale, J. H.; Almdal, K.; Mortensen, K. *Faraday Discuss.* **1994**, 7−18.
(23) Shibayama, M.; Hashimoto, T.; Hasegawa, H.; Kawai, H. *Macromolecules* **1983**, *16*, 1427−1433.
(24) Lodge, T. P.; Hanley, K. J.; Pudil, B.; Alahapperuma, V. *Macromolecules* **2003**, *36*, 816−822.
(25) Queslel, J. P.; Mark, J. E. *J. Chem. Phys.* **1985**, *82*, 3449−3452.
(26) Queslel, J. P.; Fontaine, F.; Monnerie, L. *Polymer* **1988**, *29*, 1086−1090.
(27) Mark, J. E.; Erman, B. *Rubberlike Elasticity: A Molecular Primer*; John Wiley & Sons: New York, 1988.
(28) Erman, B.; Mark, J. E. *Structures and Properties of Rubberlike Networks*; Oxford University Press: New York, 1997.
(29) Mark, J. E. *Physical Properties of Polymers Handbook*; AIP Press: New York, 1996.
(30) Hahn, H.; Chakraborty, A. K.; Das, J.; Pople, J. A.; Balsara, N. P. *Macromolecules* **2005**, *38*, 1277−1285.
(31) Gomez, E. D.; Das, J.; Chakraborty, A. K.; Pople, J. A.; Balsara, N. P. *Macromolecules* **2006**, *39*, 4848−4859.
(32) Ikkai, F.; Shibayama, M. *Phys. Rev. E* **1997**, *56*, R51−R54.
(33) Ermi, B. D.; Amis, E. J. *Macromolecules* **1997**, *30*, 6937−6942.
(34) Kim, M. H.; Glinka, C. J.; Grot, S. A.; Grot, W. G. *Macromolecules* **2006**, *39*, 4775−4787.
(35) Eitouni, H. B.; Balsara, N. P. *J. Am. Chem. Soc.* **2004**, *126*, 7446−7447.

MA0629485